

Crystal Structure of Myoglobin From a Synthetic Gene

George N. Phillips, Jr.,¹ Robert M. Arduini,¹ Barry A. Springer,² and Stephen G. Sligar^{2,3}

¹Department of Biochemistry and Cell Biology, Rice University, Houston, Texas 77251; Departments of

²Biochemistry and ³Chemistry, University of Illinois, Urbana, Illinois 61801

ABSTRACT Crystals have been grown of myoglobin produced in *Escherichia coli* from a synthetic gene, and the structure has been solved to 1.9 Å resolution. The space group of the crystals is P6, which is different from previously solved myoglobin crystal forms. The synthetic myoglobin is essentially identical to myoglobin isolated from sperm whale tissue, except for the retention of the initiator methionine at the N-terminus and the substitution of asparagine for aspartic acid at position 122. Superposition of the coordinates of native and synthetic sperm whale myoglobins reveals only minor changes in the positions of main chain atoms and reorientation of some surface side chains. Crystals of variants of the “synthetic” myoglobin have also been grown for structural analysis of the role of key amino acid residues in ligand binding and specificity.

Key words: synthetic myoglobin, X-ray crystallography, protein engineering, heme proteins

INTRODUCTION

Myoglobin binds dioxygen tightly and functions as an oxygen storage protein in muscle. This protein has been the subject of extensive biochemical and biophysical research and has served as a “prototype” for many new ideas on the behavior of proteins.^{1,2} We report here the crystal structure of myoglobin produced in *Escherichia coli* from a synthetic gene, as confirmation of the correct bacterial synthesis of the protein and as a requisite step in a mutagenesis program designed to examine the three-dimensional structural determinates that confer specificity and reactivity of ligand binding to myoglobin.

A synthetic gene for myoglobin has been constructed using overlapping fragments generated on an automated DNA synthesizer, ligated, and inserted into *E. coli* to produce copious amounts of protein.³ The bacteria provide the heme group so that active holoprotein is purified from the bacterial extracts. The myoglobin that is produced is essentially the same as myoglobin isolated from sperm whale muscle tissue, except for two known differences. Because of different posttranslational processing of proteins in bacteria and eukaryotes, the initiator methionine remains at the N-terminus of

the “synthetic” myoglobin. In addition, the codon for asparagine was inserted at the position coding for residue 122, as published in the original protein sequence determination.⁴ The amino acid at position 122 was later corrected to be aspartic acid,⁵ but this change was not taken into account in the design of the DNA. This substitution is completely benign (see below). Nevertheless, the correction at position 122 has now been incorporated in the synthetic gene. Even with the two substitutions, the synthetic “wild-type” myoglobin has been shown to be identical to native sperm whale myoglobin in terms of optical and magnetic spectroscopies,³ infrared spectroscopy and ligand dynamics,⁶ resonance Raman spectroscopy,⁷ and ligand binding kinetics.^{8–10} The obvious advantage of having myoglobin expressed in such a bacterial system is that changes in the amino acid sequence can now be easily achieved and the results correlated with changes in protein function.

The three-dimensional structure of myoglobin poses a paradox. The protein binds and releases dioxygen rapidly as its physiological function, but when the three-dimensional structure is examined there is no clear path from the solvent environment to the heme iron. The path is blocked by a layer of amino acid side chains. A major question has been which residues move to allow oxygen molecules and other ligands to get in an out of the protein.

With modification of the synthetic myoglobin gene, mutant proteins have been produced with altered ligand binding parameters.^{8–12} The substitution HisE7→Gly results in dramatic increases in the rates of ligand binding. This effect is presumably due to the removal of steric hindrance caused by the imidazole ring of the distal histidine. We have recently shown that, in the structure of myoglobin from sperm whale tissue, this residue can act as a “swinging door,” allowing ligand entry and exit when in the open configuration.¹³ ValE11 also plays a role in modulating the functional properties of myoglobin. A monotonic decrease in the association rate constants for ligands was observed when the

Received August 1, 1989; revision accepted December 11, 1989.

Address reprint requests to George N. Phillips, Jr., Department of Biochemistry and Cell Biology, Rice University, P.O. Box 1982, Houston, TX 77251.

size of the side chain at position E11 was increased from Ala to Val to Ile.¹¹ These results suggest that the distal valine also hinders access to the iron atom, although the effect is smaller than that of the distal histidine. Other mutants are also currently being characterized, including HisE7→(Val,Leu,Phe,Met,Gln,Asp,Arg), ValE11→Phe, ArgCD3→(Ser,Gly), and various "double" mutants at the E7 and E11 positions.

Several different systems are now in use for examining mutations in various myoglobins. Shimada et al.¹⁴ have expressed a bovine skeletal gene in yeast and introduced a HisE7→Arg mutation¹⁵ resulting in behavior similar to hemoglobin Zurich, which also has an Arg residue at E7; Lambright et al.¹⁶ have introduced conservative amino acid substitutions into human myoglobin expressed in *E. coli*, resulting in subtle changes in ligand binding parameters; and Dodson et al.¹⁷ have expressed a porcine myoglobin in *E. coli* for mutagenesis and crystallographic studies.

In these types of mutagenesis studies, it is important to verify that the amino acid substitutions are conservative and cause specific, localized structural effects. It is quite possible to introduce changes in a protein structure that have dramatic but purely unintentional effects. We have crystallized "wild-type" and variants of the synthetic sperm whale myoglobin, solved the high-resolution structure of the met form of the wild-type protein, and are beginning work on the high-resolution structures of both liganded and unliganded forms of the mutant proteins.

MATERIALS AND METHODS

Purification of the Proteins

The recombinant myoglobin was purified from frozen, crude, 95% saturated ammonium sulfate precipitates of cell lysates. About 50 g of the precipitate was dialyzed against 20 mM Tris HCl, 1 mM EDTA, pH 8.0 (four changes, 1 liter each), concentrated to 50 ml, and run through a DEAE-cellulose (Whatman DE-52, Clifton, New Jersey) anion-exchange column under isocratic conditions. The myoglobin fractions were then pooled; dialyzed against 20 mM sodium phosphate, 1 mM EDTA, pH 6.5; concentrated; and injected onto a weak cation-exchange semipreparative HPLC column. The myoglobin was eluted using a sodium chloride gradient and prepared for crystallization as described below. Protein prepared in this manner is homogeneous as monitored by SDS-polyacrylamide gel electrophoresis.

Crystallization

Three techniques were used to grow crystals of the synthetic myoglobin and its variants. Hanging drop vapor diffusion was used with 2.6–2.8 M ammonium sulfate in a well solution containing 20 mM Tris HCl, 1 mM EDTA, pH 9.0. A 5 μ l drop of 20 mg/ml

protein was mixed with 5 μ l of the well solution on a cover slip treated with the silanizing agent Sigma-cote (Sigma). The cover slip was inverted and sealed over the well and allowed to stand at 20°C. The second method used free interface diffusion in glass depression slides. For this method, 5 μ l of protein at 50 mg/ml was put in the well of the depression slide and brought to 2.6–2.8 M ammonium sulfate with a 3.2 M ammonium sulfate buffer solution containing 20 mM Tris HCl, 1 mM EDTA, pH 9.0. The third method was a batch technique in which 10 μ l of 70 mg/ml protein was pipetted into a 6 \times 50 mm culture tube and brought to 2.2–2.6 M ammonium sulfate with the same buffer described above. For the wild-type protein, seeding proved useful. For this procedure, several small crystals (0.2 \times 0.1 \times 0.1) were crushed in mother liquor, diluted 1 to 1,000 in the Tris buffer, and a few microliters was pipetted into the culture tubes. All three methods have produced crystals up to 0.5 \times 0.3 \times 0.15 mm size. Attempts to crystallize the protein under the same conditions we use to crystallize native sperm whale myoglobin were unsuccessful.

Collection of X-Ray Data

Space group determination was done with still and oscillation photographs on an Elliott GX-6 rotating anode with a bent quartz crystal monochromator. Initial data for the molecular replacement solution were taken by diffractometer using a Syntex P2₁ instrument and step-scan procedures. A complete data set was taken to a resolution of 3.5 Å with an R-factor for symmetry and multiple measurements of 4.5%. High-resolution data (1.9 Å) were taken on a San Diego Multiwire Systems area detector on a Rigaku rotating anode. The overall R-factor for scaling and merging all data was 5.3%, and included 50,003 measurements of 12,308 unique reflections. For the final refinement, the data from the diffractometer and the area detector were merged (R-merge of 6.7%) to help fill in some missing data in the low-resolution range. All crystals used in this study were in the oxidized, met-form as shown by optical spectra of the protein solutions prior to crystallization.

Computational Methods

Version 2.3 of the MERLOT package of programs¹⁸ was used to solve the molecular replacement problem. The translation problem was solved by direct R-factor search using the RVAMAP routine of MERLOT, after modifications were made to allow hexagonal space groups. Rigid-body refinement and molecular-dynamics refinement of the structure were done with the single precision version of the program XPLOR.¹⁹ Final refinement was done with the program PROFFT,²⁰ with electron density maps and difference maps calculated with program PROTEIN.²¹ Molecular graphics were gen-

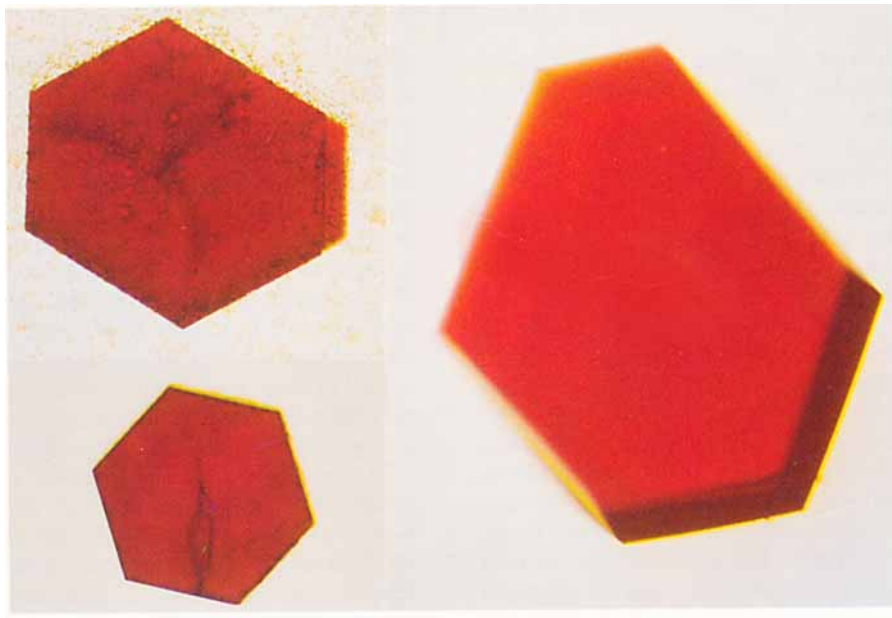


Fig. 1. Photomicrographs of crystals of myoglobin produced in *E. coli* by a synthetic gene. Crystals have been grown of various mutants, including the "wild-type" protein (**top left**), the ValE11→Phe mutant (**bottom left**), and HisE7→ Gly mutant

(**right**). The crystals grow as hexagonal plates or columns in space group P6. The crystals range in size from 0.5 to 1.0 mm in the largest dimension.

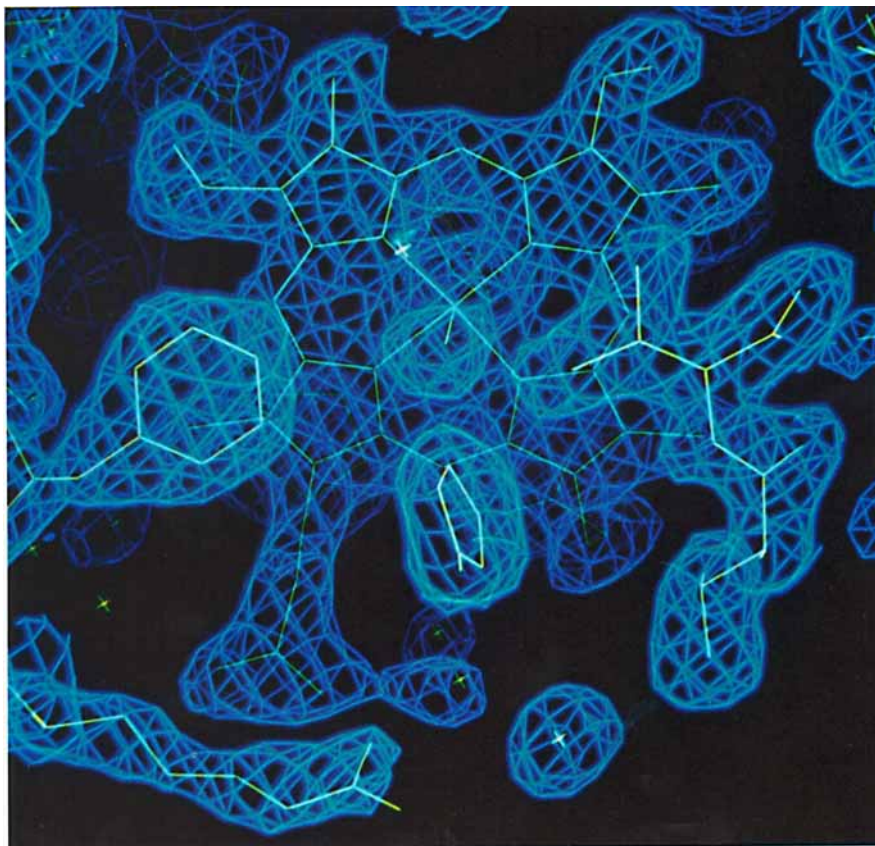


Fig. 2. 2Fo-Fc electron density map of the heme pocket, showing the properly incorporated heme and distal amino acid side chains. The hydroxide is seen bound to the iron in the center and is surrounded by Val E11, His E7 and Phe CD1 (clockwise

from right). ArgCD3 is seen at the lower left. The cross near pyrrole nitrogen II is a fractionally occupied water molecule within the binding pocket.

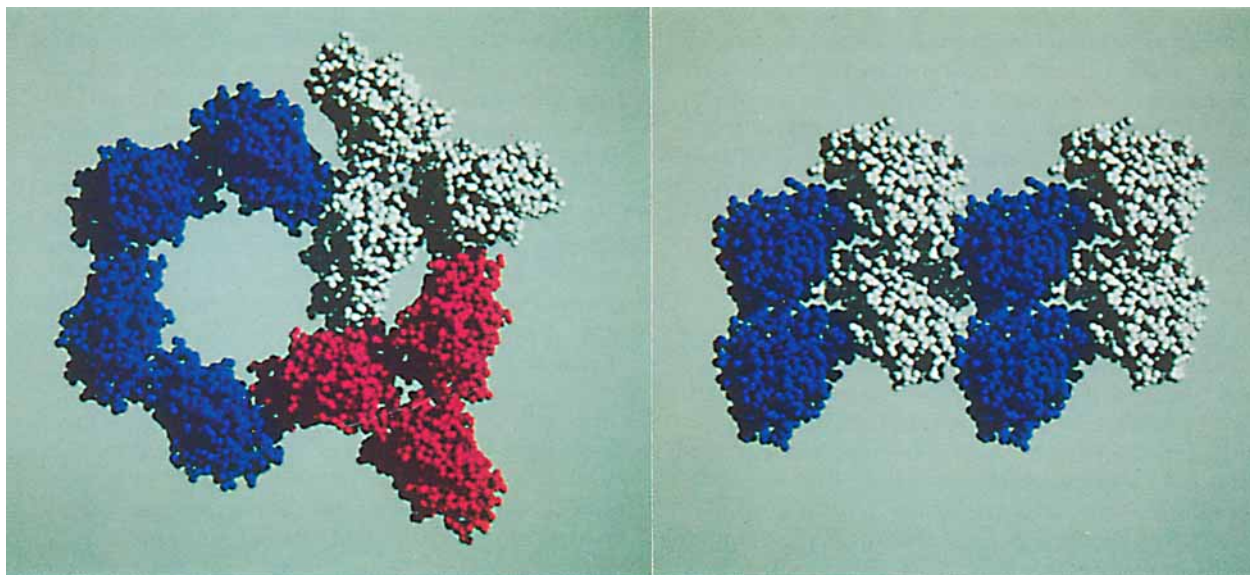


Fig. 3. Comparison of the crystal packing in two forms of myoglobin. In both space groups, the crystal is built up of layers of molecules stacked in planes approximately normal to the page. **Left:** Packing diagram of crystals of "wild-type" synthetic myoglobin in space group P6 viewed down the z-axis, with the x-axis horizontal. The molecules form tightly packed trimers around the threefold axes (white and red), with a large solvent channel

around the sixfold axes (mostly blue). **Right:** Packing of native sperm whale myoglobin in space group P2, with the y-axis vertical and the crystallographic 110 axis horizontal. The packing is generally much tighter than that in the P6 form of myoglobin. Comparison of the structure of myoglobin under these very different lattice packing constraints shows that the protein backbone folding is largely insensitive to crystal packing forces.

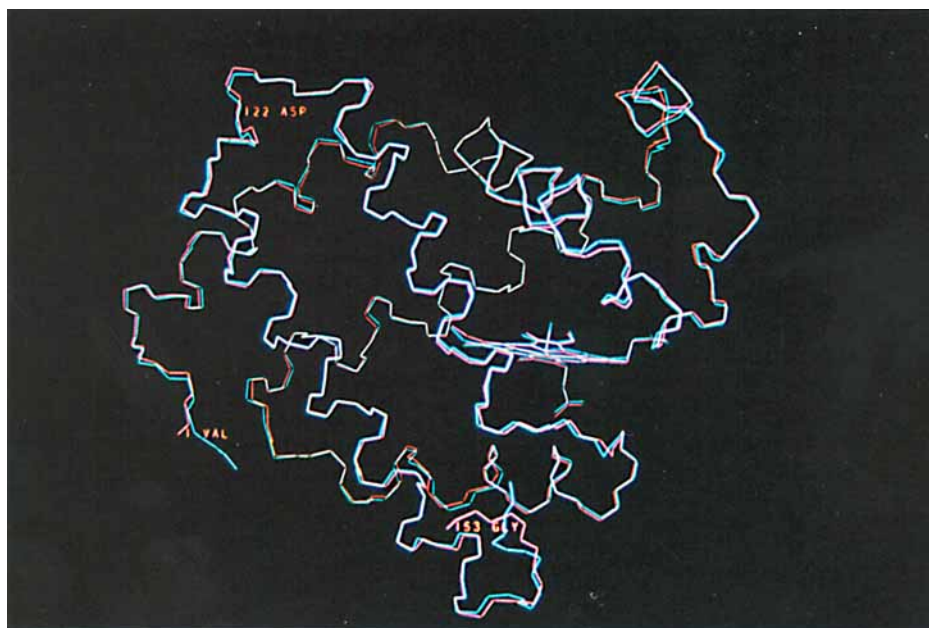


Fig. 5. Superposition of the structures of myoglobin as produced in *E. Coli* (cyan) and the native protein from sperm whale (magenta). Aside from the rearrangement of some amino acid side chains on the surface of the protein (not shown), there is a slight shift in position of the main chain atoms in the BC corner and C helix (shown just above the heme), probably due to differences in lattice packing forces. The additional initiator methionine remaining on the N-terminus of the *E. coli* myoglobin is seen at

lower left. The conformation of the carboxyl-terminus is different (bottom), but various structures have been reported for this region even amongst the various P2₁ crystal structure analyses of the protein. The region of the inadvertent Asp/Asn substitution at position 122(GH3) is shown at upper left. Generally, the structures are identical (the cyan and magenta colors superpose and appear white).

erated with PSFRODO,²² except for the packing diagrams, which used program ANIMOL (written by Richard M. Hilmer). Superpositions of molecular coordinates were carried out with subprogram U3BEST, designed and written by Kabsch.²³ All computations were carried out on a MicroVAX II or VAXstation 3200. Coordinates for the wild-type structure have been deposited with the Brookhaven Protein Data Bank.

RESULTS

Crystals of the "wild-type" and six of the variant myoglobins, including ValE11→(Ala, Ile, and Phe) and HisE7→(Gln, Leu, and Gly), have been grown in forms suitable for high-resolution structure determinations (see Fig. 1). These proteins crystallize in a different space group from the original sperm whale myoglobin crystals described by Kendrew et al.²⁴ Oscillation photographs revealed the space group to be P6, and four-circle diffractometry was used to obtain unit cell dimensions for the wild-type of $a = b = 91.2 \pm 0.1$ Å and $c = 45.87 \pm 0.06$ Å. All the crystals of the synthetic wild-type and mutant myoglobins crystallized thus far are space group P6, have identical unit cell dimensions (within 0.1–0.2 Å), and diffract to 1.7 Å resolution.

Solution of the structure of the synthetic myoglobin structure was easily achieved using the molecular replacement method. Four-circle diffractometer data to a resolution of 3.5 Å were used for this stage of the analysis. Using the coordinates for myoglobin in space group P2₁ from our study on the binding of ethyl isocyanide to sperm whale myoglobin, the Crowther rotation function gave an unambiguous peak corresponding to the final solution to within 3°. The Lattman rotation function yielded a solution within 1° of the final solution. Because there are only two independent translational variables in space group P6, the translation problem was solved using a direct R-value search procedure with grid intervals of 2 Å. Rigid-body minimization then reduced the crystallographic R-factor to 0.37.

Initial 2Fo-Fc maps at 1.9 Å resolution revealed that some side chains had changed conformations in going from the P2₁ form to the P6 form, but no changes in the positions of atoms in the protein backbone were seen. The amino terminal methionine of the synthetic protein was clearly visible and fitted to the electron density, and ten amino acid side chains on the surface of the protein were manually moved into alternate conformations. Crystallographic refinement of the starting structure was initiated with molecular dynamics coupled to crystallographic data according to the heating, quick cooling, and B-factor refinement procedures recommended by Brunger.²⁵ The R-factor was dramatically reduced from 0.34 to 0.21 with 2 days of CPU time. No improvement in R-factor was achieved using the slow cooling procedure, despite an increase

in CPU time to 6 days. In comparison, a refinement without inclusion of the molecular dynamics could reduce the R-factor only to 0.24. Electron density and difference maps were calculated, and well-ordered solvent molecules were identified. At this point, refinement was continued using restrained refinement methods to a final R-factor of 0.148, using all data from 5 to 1.9 Å and restraining the geometry to acceptable accuracy [0.02 Å root mean square (RMS) deviation in bond lengths]. Final difference maps show no significant peaks above 0.25 e/Å³. The part of the final 2Fo-Fc map including the heme and distal residues is shown in Figure 2.

The packing of myoglobin molecules in the P6 unit cell is necessarily different and much more open than in the P2₁ form (Fig. 3). The percentage solvent content in the P6 unit cell is 62%, as compared to 37% in the P2₁ cell. In the new crystal form, the molecules are packed rather tightly around the threefold crystallographic axes, but large solvent channels exist along the sixfold axes. The contact along the crystallographic z-axis includes the amino-terminal region, and this suggests that the additional N-terminal methionine is responsible for the different space group for this form of the protein, although there are also lattice contacts near residue 122, where asparagine was substituted for aspartic acid. Despite the much looser packing of molecules in space group P6, the conformation of the protein backbone is virtually identical to that in P2₁ form, confirming that crystal packing forces have had minimal effect on the overall structure of the protein.

The synthetic myoglobin has been quantitatively compared with myoglobin from sperm whale tissue. The high-resolution P2₁-form metmyoglobin structure^{26,27} has been superposed on the new crystal form using only C-alpha atomic positions and disregarding the N-terminus and the last seven residues of the sequence, which are disordered in one or the other structures. After superposition, the RMS difference in the main-chain and side-chain atomic positions between the two structures is 0.31 Å and 1.09 Å for residues 2–146, and 0.59 Å and 1.27 Å for all residues. These values indicate that, except for the N- and C-termini, there are only minor differences between the two protein structures. A plot of main chain and side chain positional differences vs. residue number is shown in Figure 4. Comparisons of residues 2–146 of synthetic myoglobin with the more highly refined coordinates of the oxy and deoxy forms of myoglobin^{28,29} from the Protein Data Bank³⁰ results in slightly smaller main-chain differences of 0.27 and 0.28 Å, despite the different oxidation and ligand states. The largest concerted difference between the P6 and P2₁ structures is a modest movement of the BC corner and C helix (residues 36–57) away from the center of the protein (Fig. 5). For an indication of the variation within

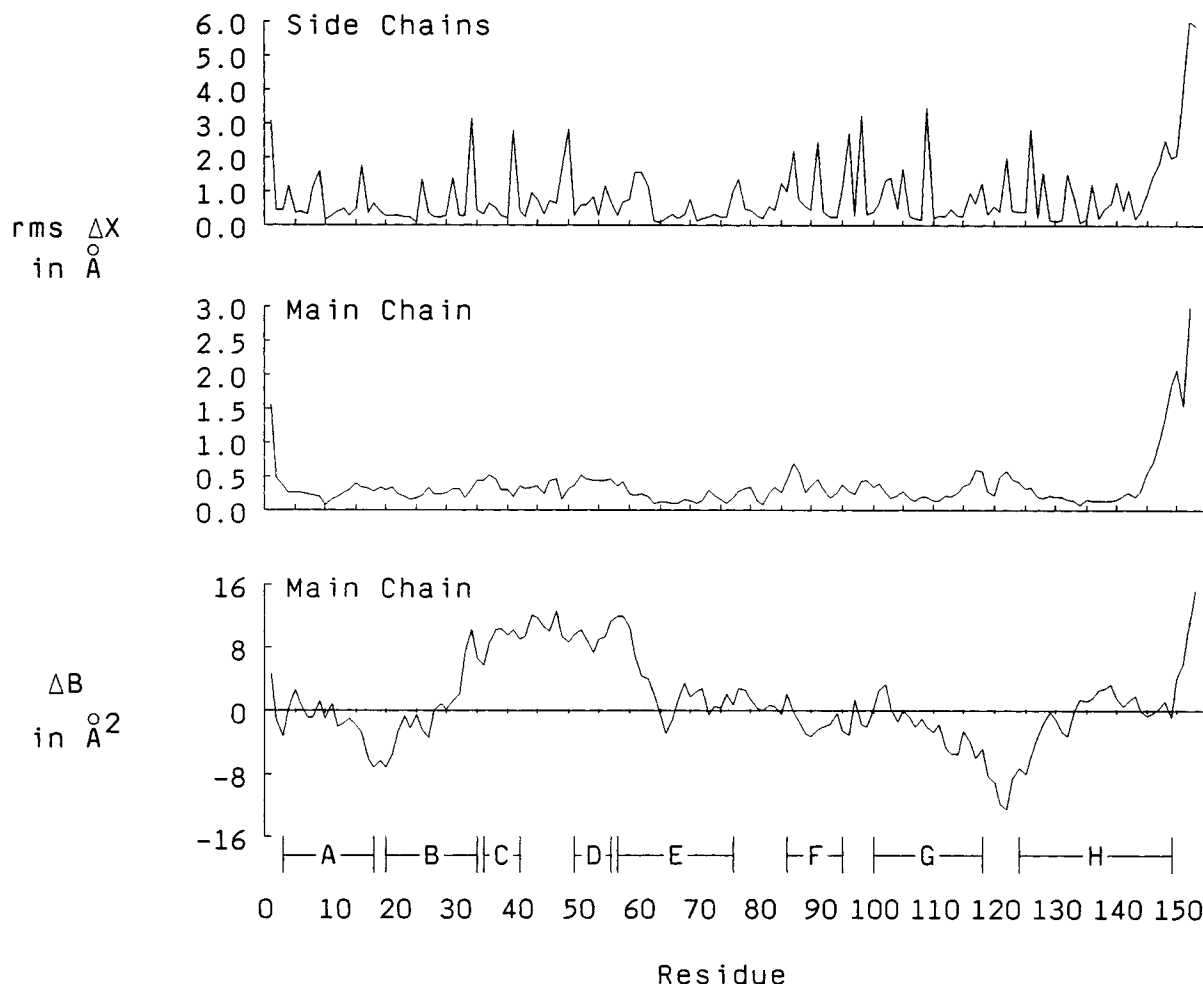


Fig. 4. Plots of the changes in positions of side chain (top) and main chain atoms (center) and changes in the crystallographic B-factors (bottom) as functions of distance along the molecule. Changes in the main-chain atom positions are minimal, except at the N-terminus and the disordered C-terminus. Some surface side chains have also adopted new conformations, but interior resi-

dues are generally unchanged. On the other hand, there are significant changes in the mobilities of certain regions of the molecule. The C helix-CD corner-D helix region is more mobile in the new P6 crystal form than the P2₁ form, and the AB and GH corners are less mobile. These changes correspond to different lattice contacts in the different crystal forms.³²

one crystal form, a value of 0.18 Å is obtained when main-chain atoms of the P2₁ forms of met-myoglobin and oxy-myoglobin are superposed.

Despite the similarity in average structure, there are some differences in the atomic mobilities in the two crystal forms (Fig. 4). A plot of the difference in B-factors between the main chain atoms of the two structures reveals that, in the P6 crystal form, residues 35–65 are more mobile than in the P2₁ form, and smaller regions near residues 15 and 120 are less mobile.

The solvent structures around the sperm whale myoglobin and the synthetic myoglobin are also similar. One sulfate ion is seen between molecules that neighbor along the crystallographic z-axis. This sulfate ion is within 2 Å of one found near residue 52 in the D-helix in the various P2₁ forms. There is, however, no ordered sulfate ion near Arg-CD3 in

this met-myoglobin structure as there is in the P2₁ met form. In addition, some water molecules have similar positions in the two crystal forms and are worthy of mention. A fractionally occupied water molecule is seen in the pocket behind the bound hydroxide, as in the oxy structure of the native sperm whale myoglobin,³¹ and two well-ordered water molecules are hydrogen bonded to the propionate groups near the entrance to the binding pocket in both the synthetic and native proteins. The role of these water molecules in determining the rates of extent of ligand binding is not yet clear.

DISCUSSION

The crystal structure presented here unambiguously confirms the proper expression of myoglobin from a synthetic gene (Fig. 2). The protein structure seen here is essentially the same as that of native

sperm whale myoglobin. After superposing the synthetic and native structures, the backbone atoms are generally overlapping, and the major difference is the orientation of side chains at the surface of the protein. Such reorientations are expected due to the different solvent conditions, intermolecular contacts, and electrostatic fields in the different lattice packing environments.

At a resolution of 1.9 Å, one might expect positional accuracies on the order of 0.1–0.2 Å. On this basis, there are a few observable differences between the P6 and the P2₁ forms, including the C-terminus, which has been reported to have a number of different conformations even within the P2₁ form of the protein, and a slight movement of the backbone atoms of the end of the BC corner and C-helix away from the heme pocket. The differences are generally small (Fig. 4), and the important point is that the overall folding of the two proteins and the orientation of key residues in the binding pocket are identical.

The effect of the two amino acid changes in the synthetic myoglobin relative to the sperm whale muscle protein is minimal. The additional N-terminal methionine lies between the F and H helices, displacing a few water molecules found in the sperm whale protein structure. The polypeptide backbone structure has not been perturbed by this addition (Fig. 4). A comparison of the two structures in the region of Asp122 also shows insignificant changes. The side chains are in slightly different conformations but the average positions of the backbone atoms are within the range of conformations reported for various liganded states of myoglobin.

A comparison of the crystallographic B-factors in the two crystal forms reveal some differences in the mobilities of certain regions of the molecule that result from the different lattice contacts (Fig. 4).³² In the P6 crystal form, the AB and GH corners of the molecule are relatively less mobile and the C helix–CD corner–D helix loop is much more mobile than in the P2₁ form. In comparing these areas, crystal packing contacts are associated with lower B-factors and hence less flexibility.³² This result contrasts with a similar study on lysozyme, in which a comparison of the structure in orthorhombic and tetragonal space groups revealed few differences in B-factors.³³ Our results indicate that lattice packing constraints do not affect the average structure of the protein much but can influence its dynamic behavior.

SUMMARY

The elucidation of this myoglobin structure shows unequivocally that protein with the correct three-dimensional structure can be produced from a synthetic gene. Any other result would have been surprising, but, nevertheless, this is the first crystal structure to be reported for a protein produced from

a totally synthetic gene. This structure will also serve as a basis for interpreting X-ray crystallographic data on engineered mutants of myoglobin.

ACKNOWLEDGMENTS

We thank John Spurlino, David Wilson, and Florante Quiocho for help with collection of area detector data; Karen Egeberg for constructing and providing ValE11 mutants; John Kuriyan for providing high-resolution sperm whale met-myoglobin coordinates, and John S. Olson for helpful discussions. This work was partially supported by NIH grants AR32764 (G.N.P.) and GM33775 (S.G.S.), NSF grant DMB-8716507 (G.N.P.), and the Robert A. Welch Foundation (C-1142) (G.N.P.).

REFERENCES

1. Perutz, M.F. Myoglobin and haemoglobin: Role of distal residues in reactions with haem ligands. *TIBS* 14:42–44, 1989.
2. Antonini, E., Brunori, M. "Hemoglobin and myoglobin and their reactions with ligands." Amsterdam: North-Holland, 1971.
3. Springer, B.A., Sligar, S.G. High-level expression of sperm whale myoglobin in *Escherichia coli*. *Proc. Natl. Acad. Sci. USA* 84:8961–8965, 1987.
4. Edmundson, A.B. Amino acid sequence of sperm whale myoglobin. *Nature* 205:883–887, 1965.
5. Romero-Herrera, A.E., Lehmann, H. Residue 122 of sperm whale and horse myoglobin. *Biochim. Biophys. Acta* 336:318–323, 1974.
6. Braunstein, D., Ansari, A., Berendzen, J., Cowen, B.R., Egeberg, K.D., Frauenfelder, H., Hong, M.K., Ormos, P., Souke, T.B., Scholl, R., Schulte, A., Sligar, S.G., Springer, B.A., Steinbach, P.J., Young, R.D. Ligand binding to synthetic mutant myoglobin (His-E7→Gly): Role of the distal histidine. *Proc. Natl. Acad. Sci. USA* 85:8497–8501, 1988.
7. Morikis, D., Champion, P.M., Springer, B.A., Sligar, S.G. Resonance raman investigations of site-directed mutants of myoglobin: Effects of distal histidine replacement. *Biochemistry* 28:4791–4800, 1989.
8. Springer, B.A., Egeberg, K.D., Sligar, S.G., Rohlfs, R.J., Mathews, A., Olson, J.S. Site-directed mutagenesis of sperm whale myoglobin: Role of His E7 and Val E11 in ligand binding. Program and Abstracts of Symposium on Oxygen Binding Heme Proteins, Asilomar, October 9–13, 1988; PII-6.
9. Olson, J.S., Mathews, A.J., Rohlfs, R.J., Springer, B.A., Egeberg, K.D., Sligar, S.G., Tame, J., Renaud, J.-P., Nagai, K. The role of the distal histidine in myoglobin and hemoglobin. *Nature* 336:265–266, 1988.
10. Springer, B.A., Egeberg, K.D., Sligar, S.G., Rohlfs, R.J., Mathews, A., Olson, S.J. Discrimination between oxygen and carbon monoxide and inhibition of autooxidation in myoglobin: Site-directed mutagenesis of the distal histidine. *J. Biol. Chem.* 264:3059–3061, 1989.
11. Egeberg, K.D., Springer, B.A., Sligar, S.G., Carver, T., Rohlfs, R.J., Olson, J.S. The role of Val⁶⁸ (E11) in ligand binding to sperm whale myoglobin, submitted.
12. Rohlfs, R.J., Mathews, A.J., Carver, T.E., Olson, J.S., Springer, B.A., Egeberg, K.D., Sligar, S.G. The effects of amino acid substitution at position E7 (residue 64) on the kinetics of ligand binding to sperm whale myoglobin. *J. Biol. Chem.*, in press.
13. Johnson, K.A., Olson, J.S., Phillips, G.N., Jr. The structure of myoglobin-ethyl isocyanide: Histidine as a swinging door for ligand entry. *J. Mol. Biol.* 207:459–463, 1989.
14. Shimada, H., Fukasawa, T., Ishimura, Y. Expression of bovine myoglobin cDNA as a functionally active holoprotein in *Saccharomyces cerevisiae*. *J. Biochem.* 105:417–422, 1989.
15. Shimada, H., Dong, A., Matsushima-Hibiya, Y., Ishimura, Y., Caughey, W. Distal His→Arg mutation in bovine myoglobin results in a ligand binding site similar to the ab-

- normal beta site of hemoglobin Zurich ($\beta 63 \text{ His} \rightarrow \text{Arg}$). *Biochem. Biophys. Res. Commun.* 158:110–114, 1989.
16. Lambright, D.G., Balasubramanian, S., Boxer, S.G. Ligand and proton exchange dynamics in recombinant human myoglobin mutants. *J. Mol. Biol.* 207:289–299, 1989.
 17. Dodson, G., Hubbard, R.E., Oldfield, T.J., Smerdon, S.J., Wilkinson, A.J. Apomyoglobin as a molecular recognition surface: Expression, reconstitution and crystallization of recombinant porcine myoglobin in *Escherichia coli*. *Protein Eng* 2:233–237, 1988.
 18. Fitzgerald, P.M.D. MERLOT, an integrated package of computer programs for the determination of crystal structures by molecular replacement. *J. Appl. Crystallogr.* 21: 273–278, 1988.
 19. Brunger, A., Karplus, M., Petsko, G.A. Crystallographic refinement by simulated annealing: Application to crambin. *Acta Crystallogr.* A45:50–61, 1989.
 20. Finzel, B.C. Incorporation of fast Fourier transforms to speed restrained least-squares refinement of protein structures. *J. Appl. Crystallogr.* 20:53–55, 1987.
 21. Remington, S., Wiegand, G., Huber, R. Crystallographic refinement and atomic models of two different forms of citrate synthase at 2.7 Å and 1.7 Å resolution. *J. Mol. Biol.* 158:111–152, 1982.
 22. Pflugrath, J.W., Saper, M.A., Quijcho, F.A. In: "Methods and Applications in Crystallographic Computing." Hall, S., Ashida, T., eds. Oxford: Clarendon Press, 1984:404–407.
 23. Kabsch, W. A solution for the best rotation to relate two sets of vectors. *Acta Crystallogr.* A32:922–923, 1976.
 24. Kendrew, J.C., Parrish, R.G., Marrack, J.R., Orlans, E.S. The species specificity of myoglobin. *Nature* 174:946–948, 1954.
 25. Brunger, A. XPLOR (Version 1.5) Manual. 1988:128–132.
 26. Kuriyan, J. Structure and flexibility of myoglobin: X-ray crystallography and molecular dynamics studies. Ph.D. Thesis, Massachusetts Institute of Technology, 1986.
 27. Frauenfelder, H., Hartmann, H., Karplus, M., Kuntz, I.D., Jr., Kuriyan, J., Parak, F., Petsko, G., Ringe, D., Tilton, R.F., Jr., Connolly, M.L., Max, N. Thermal expansion of a protein. *Biochemistry* 26:254–261, 1987.
 28. Entry 1MBD, Brookhaven Protein Data Bank.
 29. Entry 1MBO, Brookhaven Protein Data Bank.
 30. Abola, E.E., Bernstein, F.C., Koetzle, T.F., Williams, G.J.B., Meyer, E.F., Brice, M.K.D., Rodgers, J.R., Kennard, O., Shimanouchi, T., Tasukmi, M. In: *Crystallographic Databases—Information Content, Software Systems, Scientific Applications*. Allen, F.H., Bergerhof, G., Sievers, R., eds. Bonn/Cambridge/Chester: Data Commission of the Int'l Union of Crystallography, 1987:107–132.
 31. Phillips, S.E.V. Structure and refinement of oxymyoglobin at 1.6 Å resolution. *J. Mol. Biol.* 142:531–554, 1980.
 32. Phillips, G.N., Jr. Comparison of the dynamics of myoglobin in different crystal forms. *Biophys J.* 57:381–383, 1990.
 33. Artymiuk, P.J., Blake, C.C.F., Grace, D.E.P., Oatley, S.J., Phillips, D.C., Sternberg, M.J.E. Crystallographic studies of the dynamic properties of lysozyme. *Nature* 280:563–568, 1979.